

VALIDATION OF TREATMENT PLANNING AND LUNG DOSE
ESTIMATION FOR TOTAL BODY IRRADIATION USING THE
ECLIPSE TREATMENT PLANNING SYSTEM

By

Mason W. Heath

A THESIS

Presented to the Medical Physics Graduate Program
and the Oregon Health & Science University
School of Medicine
in partial fulfillment of
the requirements for the degree of

MASTER OF SCIENCE

May 2022

Table of Contents

LIST OF FIGURES.....	II
LIST OF TABLES	III
ABBREVIATIONS.....	IV
ACKNOWLEDGMENTS	V
ABSTRACT.....	VI
1. INTRODUCTION.....	1
2. BACKGROUND AND MATERIALS.....	5
2.1 TOTAL BODY IRRADIATION	5
2.2 PHANTOM	7
2.3 TREATMENT PLANNING	9
2.4 FILM DOSIMETRY	9
2.5 ION CHAMBER DOSIMETRY	10
3. METHODS	12
3.1 TBI PROTOCOL	12
3.2 PATIENT SELECTION	13
3.3 PHANTOM SETUP	13
3.4 ECLIPSE TREATMENT PLANNING	14
3.5 HAND CALCULATIONS	18
3.6 LUNG BLOCK FABRICATION	19
3.7 ION CHAMBER DOSIMETRY	21
3.7.1 Chamber Calibration	21
3.7.2 Stem and Cable Effects.....	22
3.7.3 Ion Chamber Phantom Measurements	23
3.8 FILM DOSIMETRY	24
3.8.1 Film Calibration	24
3.8.2 Phantom Measurements.....	25
3.8.3 Film Processing.....	28
4. RESULTS.....	30
5. DISCUSSION	35
5.1 FINDINGS.....	35
5.2 LIMITATIONS & FUTURE WORK.....	38
6. SUMMARY AND CONCLUSION	40
WORKS CITED	42

List of Figures

FIGURE 1: ELEKTA VERSA HD™ USED BY OHSU AND THIS STUDY FOR THE DELIVERY OF TBI TREATMENTS.	5
FIGURE 2: SCHEMATIC OF TYPICAL TBI SETUP. THIS INCLUDES THE TRAY WHERE MISSING TISSUE COMPENSATION WOULD BE PLACE, THE LUNG BLOCKS PLACED ON THE DEGRADER, THE DEGRADER AT 510 CM, AND THE PATIENT LOCATED AT THE PRESCRIPTION DISTANCE OF 562.5 CM FROM THE SOURCE TO THE MID BODY.	6
FIGURE 3: PHANTOM CONSTRUCTED OUT OF SOLID WATER AND CEDAR PLANKS USED FOR TREATMENT PLANNING.	8
FIGURE 4 SETUP OF PHANTOM USED IN FILM AND ION CHAMBER DOSIMETRY AS WELL AS IN TPS AND HAND CALCULATIONS. LABELED WITH INFERIOR AND SUPERIOR SIDES THAT ARE REFERENCED AS WELL AS SOME DIMENSIONS OF TOTAL THICKNESS AND THICKNESS OF CEDAR SECTION.	14
FIGURE 5: CONTOUR OF LUNGS IN BLUE AND CONTOUR OF LUNGS MINUS 1.5 CM MARGIN IN GREEN WITH REFERENCE POINTS CENTERED IN BOTH RIGHT AND LEFT LUNGS.	15
FIGURE 6: CROSS-SECTION OF TBI PHANTOM WITH LUNG CONTOUR IN BLUE AND LUNG CONTOUR -1.5CM IN ORANGE AS WELL AS MID LUNG AND MID BODY REFERENCE POINTS.	16
FIGURE 7: EXAMPLE OF THE ORIENTATION OF THE LUNG BLOCKS WITH RESPECT TO PATIENT BODY. CERROBEND BLOCKS ARE ALIGNED TO THE LUNGS USING CR IMAGING TECHNIQUES AND PLACED ON THE SPOILER AT A DISTANCE OF 510 CM FROM THE SOURCE DURING BEAM DELIVERY.	17
FIGURE 8: SIMILAR TRIANGLES DIAGRAM.	20
FIGURE 9: EXAMPLE OF PRINTED LUNG BLOCK TEMPLATE USED TO CREATE BLOCK FORMS SHOWN IN ORANGE AND GRATICULE LINES IN YELLOW.	21
FIGURE 10 MEASUREMENT OF CHARGE WITH THE STEM AND CABLE IN THE FIELD DURING IRRADIATION TO VERIFY THE SIGNIFICANCE OF STEM AND CABLE EFFECTS. NOT VISIBLE IN THE PHOTO, THE FARMER CHAMBER IS PLACED AT THE CENTER OF THE FIELD AT A DEPTH OF 3CM. THE DOSE WAS NOT DERIVED FROM THIS READING. THE CHARGE READING WAS COMPARED WITH AND WITHOUT THE CABLE IN THE FIELD.	23
FIGURE 11: THE TBI PHANTOM WITH THE LUNG AND BODY SECTIONS LABELED. THE YELLOW ARROWS INDICATE THE PATH OF THE BEAM THROUGH THE PHANTOM.	24
FIGURE 12: ONE OF THE FILMS USED FOR REFERENCE DOSIMETRY DURING THE PROCESSING OF THE STRIPS PLACED IN TBI PHANTOM. THIS FILM WOULD THEN HAVE 3.2CM OF SOLID WATER PLACED ON TOP AND IRRADIATED TO ONE OF THE LISTED CALIBRATION DOSE LEVELS. THIS SETUP WAS ALSO USED FOR SUBSEQUENT TRIALS TO VERIFY THE ACCURACY OF THE INITIAL REFERENCE DOSE TO AVOID CREATING NEW DOSE CONVERSION FILES FOR READING ON SEPARATE DAYS.	25
FIGURE 13: THE CALIBRATION FILMS ARE SHOWN WITH ARROW MARKINGS INDICATING INITIAL ORIENTATION WHEN REMOVED FROM FACTORY PACKAGING. THESE ARROWS ARE USED TO MAINTAIN CONSISTENT ORIENTATION WHILE BEING SCANNED.	27
FIGURE 14: THE TBI PHANTOM IS POSITIONED FOR IRRADIATION. IN THE BEAM PATH IS THE CERROBEND BLOCK POSITIONED TO SHIELD THE CENTRAL PORTION OF THE SUPERIOR SECTION OF THE PHANTOM. THE BLOCK PICTURED IS THE RECTANGULAR DESIGN CREATED FOR THE PLAN CREATED DIRECTLY ON THE TBI PHANTOM. THE BLOCK IS FASTENED TO THE ACRYLIC SPOILER USING VELCRO ATTACHED TO A MOUNT AT AN SSD OF 510 CM.	27
FIGURE 15: PICTURED IS A SIDE VIEW OF THE TBI PHANTOM WITH THE LOCATION OF THE FILM PLACEMENT REPRESENTED BY RED MARKERS. FILM SIZE VARIED BUT THE UPPER TWO MARKS SHOW THE LOCATION OF THE LARGER FILMS USED TO GET PROFILES OF BLOCKED FIELDS. THE LOWER MARKER REPRESENTS THE LOCATION OF THE SMALLEST FILM USED THAT MEASURES THE DOSE AT THE PRESCRIPTION POINT.	28

List of Tables

TABLE 1: LIST OF VARIABLES USED FOR HAND CALCULATIONS IN TBI TREATMENT PLANNING.....	19
TABLE 2: TABULATION OF BEAM ENERGY, PATIENT SETUP, SHIELDING USED, PATIENT SEPARATION, AND LUNG VOLUME FOR EACH PATIENT AND PATIENT PLAN CREATED IN THE TPS AND FOR HAND CALCULATIONS. THE LUNG VOLUME FOR PATIENT 9 ^{††} IS THE RECTANGULAR CONTOUR OF THE TBI PHANTOM.....	30
TABLE 3: STEM AND CABLE EFFECTS FOR 6MV AND 18MV BEAMS WHEN USING THE FARMER CHAMBER. THE PERCENT REPORTED IS THE MEAN INCREASE IN CHARGE COLLECTION WHEN THE CABLE IS ADDED TO THE FIELD.	31
TABLE 4: PERCENT DIFFERENCE OF DOSE MEASURED BY THE FARMER ION CHAMBER AT THE PRESCRIPTION POINT WITH A VARYING PHANTOM THICKNESS TO THE DOSE PREDICTED BY HAND CALCULATIONS (75 cGy) ON THE TBI PHANTOM. THE PHANTOM THICKNESS WAS ADJUSTED TO MATCH A PATIENT’S THICKNESS FROM THE TPS PLANS.	31
TABLE 5: TOTAL MONITOR UNITS PREDICTED PER FIELD FROM BOTH THE ECLIPSE ACUROS [®] ALGORITHM AND USING HAND CALCULATION METHODS WITH A PERCENT DIFFERENCE OF ECLIPSE [™] MUs FROM THAT BY HAND CALCULATIONS. THE ACUROS [®] PREDICTION VARIED SLIGHTLY BETWEEN AP AND PA BEAMS SO THE AVERAGE OF THE TWO WAS TAKEN.....	32
TABLE 6: DIFFERENCE IN LUNG DOSE PREDICTIONS WITHOUT LUNG SHIELDING BY ECLIPSE ACUROS [®] ALGORITHM FROM HAND CALCULATION PREDICTIONS.	32
TABLE 7: COMPARISON OF DOSE MEASURED IN LUNG REGION WITHOUT LUNG BLOCKS WITH ECLIPSE [™] CALCULATED DOSE ON TBI PHANTOM FOR AN 18MV BEAM	33
TABLE 8: PERCENT DIFFERENCE OF BLOCKED LUNG DOSE AND MID BODY DOSE MEASUREMENTS FROM FILM ON THE TBI PHANTOM COMPARED TO CALCULATED VALUES BY THE ECLIPSE ACUROS [®] ALGORITHM.	33
TABLE 9: COMPARISON OF MEAN TO MID LUNG DOSE CALCULATED BY THE ECLIPSE ACUROS [®] ALGORITHM ON PATIENT CT SIM DATA OF PATIENT PLANNED IN THE APPA BEAM DIRECTION SETUP. THESE COMPARISONS ARE OF DOSE ACCUMULATED FROM ALL FRACTIONS IN THE PLAN INCLUDING BLOCKED AND UNBLOCKED FIELDS.	34
TABLE 10: COMPARISON OF MEAN TO MID LUNG DOSE CALCULATED BY THE ECLIPSE ACUROS [®] ALGORITHM USING INFORMATION FROM CT SIM IMAGES OF PATIENTS PLANNED IN THE LATERAL BEAM DIRECTION SETUP. THESE ARE COMPARISONS OF DOSE ACCUMULATED FROM ALL FRACTIONS OF THE TREATMENT PLAN.	34

Abbreviations

APPA	Anterior-Posterior/Posterior-Anterior
CR	Computed Radiography
CT	Computed Tomography
d_m	Depth of Dose Maximum
LBTE	Linear Boltzmann Transport Equation
MV	Maximum Beam Energy in MeV
MU	Monitor Unit
ROI	Region of Interest
Sim	Simulation
SSD	Source to Surface Distance
TBI	Total Body Irradiation
TPS	Treatment Planning System
WED	Water Equivalent Distance

Acknowledgments

I'd like to first acknowledge my advisor Sussha Pillai. Through a busy clinical schedule, she has made an extreme effort to make herself available. Her expert opinion and input was critical to the completion of this project.

I'd also like to thank the other members of my committee, Dr. Junan Zhang and Dr. Anna Mench, for their contributions to this project and the time and preparation they put in for my thesis defense.

I'm grateful to all of the faculty and staff of OHSU radiation medicine, who have taken us students under their wing and gone above and beyond in preparing us to be impactful in our careers. The department supplied all equipment including one of their linacs as well as dosimetry supplies for this project.

I'm extremely appreciative of my cohort. Making it through graduate school during a pandemic was no easy task. The bonds we've made helped make expectations feel more manageable. From late nights out to the late-night homework sessions, without them, I would not have been successful in this endeavor.

I'd also like to thank my friends and family for their continual love, support, and sacrifices that have allowed me to devote myself to this academic journey. Sometimes it feels like an endless path and I couldn't imagine taking it alone.

Abstract

The lungs are the primary dose limiting organ in high dose total body irradiation (TBI). Accurate prediction of lung dose can dictate treatment success by preventing pulmonary toxicity. Normal treatment planning consists of basic hand calculations and potentially *in vivo* dosimetry. The use of a treatment planning system (TPS) is an unverified method at the extended treatment distance required by TBI. In this study, we attempted to analyze the Eclipse TPS for used in a TBI setup. Both its ability to determine the required monitor units (MU) and its ability to compensate for tissue heterogeneity in lung dose estimates were compared to traditional techniques and dosimetry.

For standard hand calculations, MU predictions are solely dependent on patient thickness. The Eclipse TPS uses the Acuros algorithm to calculate MU's using patient-specific anatomy information. The TPS provides a more complex dose distribution that allows for the extraction of both a point dose estimate as well as volume-based information like a mean dose to the lungs. A phantom that mimics the densities in the human trunk, with sections specific to the lungs and abdomen, was irradiated using patient plan information. Dosimetry measurements in the phantom were compared to both the TPS and hand calculation predictions.

Like all radiotherapy, careful treatment planning can have a dramatic effect in treatment success for TBI. A change in lung dose as little as 5% can have a pronounced effect on patient complications. Typically, a point dose is used during planning in all locations because of its convenience and ease of calculation. Estimations by Eclipse™ show this may be an inaccurate method especially in the lungs where shielding causes

large dose variations. Examination of TPS predictions show mean lung dose is as much as 14% higher than the mid lung point dose estimates in plans that incorporate shielding.

Dose estimation by the TPS for unshielded locations has been in line with clinical expectations. The dosimetry measurements at the prescription point (mid body) were all within $\pm 2\%$ of the TPS prediction. In a more heterogeneous material like the lungs, the mean difference was near 3% before incorporating shielding.

Using current TPS planning techniques, fields using lung shielding show large differences from measured quantities. These are significantly higher and can't yet be implemented into a planning procedure. Developing a new planning technique may overcome this deficit.

Differences in shielding measurements are too large to be incorporated into a planning procedure. In the contrary, dose estimation regardless of heterogeneity show clinically relevant accuracy. These initial results suggest it could be a valuable predictor prior to implementing shielding though further investigation is warranted. If future work is able to overcome the challenges faced with implementing shielding, the TPS could be a valuable tool for complete TBI treatment planning.

1. Introduction

Total body irradiation (TBI) is a special high-dose procedure in radiotherapy. Combined with intensive chemotherapy, TBI is an effective and often critical tool in hematopoietic stem cell therapy. Used to treat a broad range of diseases, it is a common preparatory step in the treatment of malignancies such as leukemia, non-Hodgkin's lymphoma, and neuroblastoma [1].

The target of TBI is the entirety of the body with special considerations being made to ensure even the skin receives an acceptable dose. At the dose levels achieved, there are organs at risk (OAR) that need appreciable considerations to avoid toxic effects. In conjunction with chemotherapy and other prophylactic treatments, the functionality of critical structures must be maintained. In a parallel organ architecture like the lungs, this means that a sufficient portion of its volume must remain functional [2].

Several delivery methods have been developed to provide a TBI treatment with wide variations from clinic to clinic. In many cases, a standard linear accelerator (linac) is used at an extended distance. This extended distance allows for a field size to exceed the scattering volume and contain the entirety of the body [3]. The current recommendation by AAPM Task Group 29 is to deliver a dose within $\pm 5\%$ [4]. A variety of more current publications state that a $\pm 10\%$ is acceptable [1 5]. Both recommendation have drawn criticism because with a 5% difference in dose fatal lung pneumonitis incidences can vary as much as 20% [4]. Historically there has been a wide variation in both dose and fractionation for the prescription of TBI. Currently, it's typical to deliver a total dose between 10 to 14 Gy to the mid body at the umbilicus delivered in multiple fractions per day for multiple days [4]. At OHSU, this is typically 2 fractions per day for up to 4 days.

The dose delivered to the lungs, as well as the dose rate, is one of the limiting factors in a TBI treatment. This requires special considerations to decrease the probability of fatal pulmonary toxicity. Various methods have been used to quantify the dose to the lungs. Radiochromic film has been used in some instances to provide a two dimensional retrospective approximation [6]. Simplicity has justified the use of a point dose estimate accompanying *in vivo* measurements during treatment, although dose monitoring has not been standardized. Because of the inconsistencies in treatment methods, it has been difficult to make exact dose recommendations. There is evidence for severe pulmonary complications at a dose as low as 8 Gy with a typical dose rate of 10-12 cGy/min to the whole lung [7].

Simple methods are employed to keep lung dose to an acceptable level. During TBI treatment, lung shielding usually made from cerrobend, called lung blocks, is sometimes used for beam attenuation for part of the treatment course. These lung blocks are often based on lung contours from computed tomography (CT) simulation (sim) images. They are placed in the beam path and designed to fit the exterior of the lung contour and are scaled for beam divergence. The blocks are typically aligned to the lungs using computed radiography (CR) port film. This can be placed behind the patient opposite the side of the linac and exposed to a small dose. This forms an image that visualizes both the lung blocks and the lungs.

If the beam directions are oriented lateral to the patient, it is common to not incorporate lung shielding. Extra tissue from the shoulders and around the lungs provide attenuation that can decrease lung dose, though its effectiveness is scrutinized. The more

pressing concern is to not underdose these extra tissues that surround the lungs in this direction which could risk insufficient cancer cell killing in these locations [8].

Treatment planning becomes more problematic when the distance from the source is extended past standard clinical practices. A typical source-to-surface distance (SSD) for radiotherapy is around 100 cm. In TBI, SSD is extended 4 to 6 times farther depending on an individual clinic's available space and preference[9]. As indicated before, this is to encompass the entirety of the patient's body within a static open field from a linac. Precise dose calculations are imperative in TBI to reduce the risk of injury from over irradiation of critical structures or complications such as rejections of donor bone marrow or survival and spreading of malignancies from an under-delivery of dose.

Typical radiotherapy would use a treatment planning system (TPS) to predict the complex dose distribution. These systems are designed and commissioned for calculations within the aforementioned typical SSD of around 100 cm and not the extended SSD of TBI [9]. Convenience and simplicity have justified the use of a point dose estimate over a more complex calculation. Point dose estimates are useful when making a prescription and provide some quantification of the dose homogeneity between different sites. They lack the ability to account for tissue heterogeneity and fail to provide more complex dose distribution information in three dimensions. These factors can be imperative in evaluating dose to critical structures [9].

Evaluation of TBI methods has proven to be difficult in previous studies. Lack of standardization and accurate prediction of complex dose distributions have prevented previous studies from drawing clear conclusions on TBI research. It is critical that the dose to the lungs is considered and is partly indicative of treatment success. In this study,

we evaluate the ability of the Eclipse treatment planning system's accuracy to predict the dose distribution in both a homogeneous and heterogeneous material. This is comparable to scattering condition encountered in both the tissues within and around the lungs and in the abdomen. The treatment model used by Oregon Health and Science University's radiation medicine department was used as a basis for the experimental outlines of this thesis.

2. Background and Materials

2.1 Total Body Irradiation

High-dose total body irradiation is a special procedure in radiation therapy. TBI is a common technique to destroy bone marrow and suppress leukemic cells for a variety of diseases [4]. A variety of techniques have been developed to administer TBI that depends on the resources available to a clinic[4]. In many cases, treatment is planned using a standard therapeutic linear accelerator (linac).



Figure 1: Elekta versa HD™ used by OHSU and this study for the delivery of TBI treatments.

At OHSU, the primary linac used for TBI and the one used for this study is their Elekta versa HD™. The linac has a maximum square field size of 40 cm in each direction at an SSD of 100 cm. For TBI, the patient is required to have complete coverage from head to toe by the radiation field. In order to achieve this coverage, the treatment distance is extended much further. At OHSU, the collimator is also rotated to 45° and the gantry is set to 90°. The standard prescription point is at a distance of 562.5 cm from the source to mid body at the level of the umbilicus. This is the largest distance allowed by the room

geometry. Accounting for beam divergence, this gives a field size of 225 cm in each direction. With the collimator rotated, there is 318cm of coverage from corner to corner of the radiation field. This is sufficient to cover most patients that are placed in the decubitus position.

A 1.5 cm spoiler is placed in the beam path at 510 cm from the source. The spoiler is made of acrylic and increases electron contamination. Increased electron contamination then increases the dose in the buildup region [4]. The spoiler also serves as a mount for the lung shielding. The lung blocks are custom shaped to the patient's anatomy and are made of cerrobend, a metal alloy. This alloy is 50% bismuth, 26.7% lead, 13.3% tin, and 10.0% cadmium with a density around 83% that of lead [10]. The use of lung blocks and other compensation is dependent on patient setup.

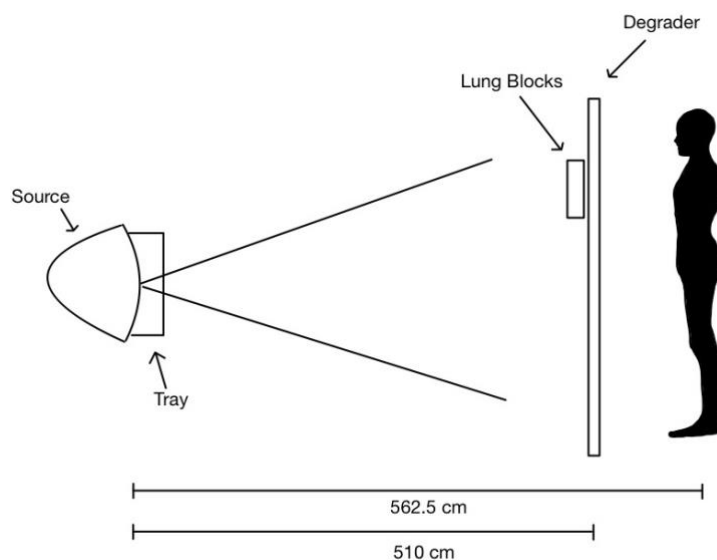


Figure 2: Schematic of typical TBI setup. This includes the tray where missing tissue compensation would be place, the lung blocks placed on the degrader, the degrader at 510 cm, and the patient located at the prescription distance of 562.5 cm from the source to the mid body.

In real patient treatments, missing tissue compensation is added to the beam path. This is to increase dose homogeneity in regions of decreased thickness and is commonly

made from brass, lead, lead alloys or other materials. Missing tissue compensation was not incorporated into our plans or measurements for simplicity purposes.

To increase dose homogeneity to within a $\pm 5\%$ total body variation, higher energy megavoltage x-rays are preferred [4]. At OHSU, adult patients are treated with an 18 MV beam. For pediatric patients, it's possible to achieve the necessary homogeneity at a lower energy and thus 6 MV is a common choice. At OHSU, the linac used for TBI is commissioned for 6, 10, and 18 MV photon beam energies and each was incorporated to some extent in our measurements.

2.2 Phantom

Radiation interactions in water are similar to those in the human body. Because of this, dose in water has become a standard reference in radiotherapy. In many circumstances, it is impractical and difficult to set up a water tank that would normally be used in annual quality assurance for a linac. In many cases, solid water can be substituted. Solid water is an epoxy-resin based material chemically doped such that it has a similar relative density to water [11]. Dosimetry in solid water has minimal differences from that in water and no corrections for density or composition are required for megavoltage x-ray beams [11]. For this reason, it is considered a good substitute for quick measurements.

For the particular dosimetry measurements in many of our experiments, a phantom approximately resembling human anatomy was needed. Specifically, a lower density portion to represent the lungs and a more water equivalent density section to represent the human abdomen. A simple phantom was constructed using solid water and cedar planks. The CT number of the cedar planks is near -700 HU. This was thought to

be a good substitute for lung tissue which is primarily composed of air and soft tissue and has a CT number between -950 and -700 HU [12].

The cedar planks measured $27\text{ cm} \times 29\text{ cm} \times 3\frac{2}{3}\text{ cm}$. Shown below, 3 of these cedar planks were sandwiched between 7 cm of solid water on each side resulting in a 25 cm thick section. This section of the phantom is meant to model the density of the thorax and represent tissue heterogeneities encountered in this anatomy. The abdomen is modeled by a 25 cm thick region of solid water. The thickness of the abdomen section was modified for some measurements and is indicated in the methods section. Each solid water slab seen below has a square cross-section of 30 cm in each direction. The purpose of this phantom was not to identically mimic human anatomy like an anthropomorphic phantom but to provide a good approximation for the scattering conditions of the human trunk.



Figure 3: Phantom constructed out of solid water and cedar planks used for treatment planning.

2.3 Treatment Planning

The gold standard for dose calculations in radiotherapy is Monte Carlo algorithms. These algorithms use a stochastic approach to solve the linear Boltzmann transport equation (LBTE) that can theoretically calculate the exact dose distribution from a radiotherapy treatment [13]. Monte Carlo methods are not currently the standard in radiotherapy because the computational resources they require are too time consuming. Instead, vendors have turned to simplified algorithms that are more feasible in the clinic. One of the more recent dose calculation algorithms currently implemented is the Eclipse Acuros® XB. This uses a grid-based approach that uses discrete photon and electron fluences that gives a deterministic solution to the LBTE [13]. At OHSU, this is the preferred dose calculation method and was used for all calculations in this study.

Dose algorithms are reliant on CT images for attenuation and scattering information. A lookup table is used to equate electron density to the Hounsfield Units (HU) from the CT images. The electron density is directly proportional to probability of interaction for each x-ray energy and is used in dose calculations[14]. In most cases the first step of a TPS plan is to obtain CT images. At OHSU, the Phillips CT Big Bore, which is designed for CT sim, was used to acquire these images. Patient images were acquired during their treatment course as part of their typical treatment planning.

2.4 Film Dosimetry

Film dosimetry is a type of reference dosimetry that requires calibration to a known dose. Radiation interactions cause a chemical reaction within the film that results in polymerization and an increase in optical density (OD) [15]. The OD change can be measured using a flatbed scanner and compared to reference measurements. For this

study, the Epson® Expression 10000xl A3 Flatbed Graphic Arts Scanner with the red color channel selected was used for all film reading. This allowed for 48-bit resolution and 72 dpi. Subsequent image files were analyzed using the Varian product DoseLab Pro which is a software developed for film quality assurance (QA) testing.

This study uses GAFchromic™ type EBT-3 film, a type of radiochromic film. For photons in the keV and MeV range, this type of film shows insignificant energy dependence [16]. This allows for cross-calibration of films irradiated with separate photon beam energies in the megavoltage range. In this study, two energies were analyzed using film, 6 MV and 18 MV.

Several studies have investigated the stability and reproducibility of GAFchromic™ film. Many have noted dramatic changes in optical density within the first hour of irradiation. After 4 hours post-irradiation, it has been noted that the optical density changes as little as 0.1 %/min [17]. Similar results have been observed between different generations of GAFchromic™ film [17]. When wait periods are extended, noise begins to reduce in the film. The greatest OD stability is observed after 24 hours post irradiation [18]. This has become the standard wait period recommendation [18]. Faster procedures have been suggested and implemented. If a consistent wait period is used, reproducible results are achievable [17].

2.5 Ion Chamber Dosimetry

Ion chamber dosimetry is another type of reference dosimetry. Ion chambers come in various shapes and sizes but are the simplest form of gas-filled detector. They measure the charge created when ionizing radiation passes through a gas [19]. This charge collection is dependent on the applied electric field to a chamber. The most

common operation mode of an ion chamber is in the ion saturation range. This is when the voltage across the chamber is high enough to prevent recombination of ions produced by the radiation but not so large that gas multiplication occurs [19]. In this mode of operation, the dose delivered is equivalent to the charge collected.

In clinical applications of an ion chamber, it's critical to obtain a charge to dose conversion factor. This is usually obtained by referencing to calorimetry measurements in a cobalt-60 beam [2]. This reference dosimetry is performed by an accredited dosimetry calibration laboratory (ADCL). The ion chamber calibration comes with a conversion factor from a cobalt-60 beam to the energy of a linac that is used to convert charge to dose. The linac is then calibrated according to a clinic's protocol to emit a specified dose under specific conditions. Further details can be found outlined in TG-51 by AAPM [2].

At OHSU, the protocol for linac calibration is to deposit 1 cGy/MU at depth maximum (dm) in water for a 10 cm x 10 cm square field at an SSD of 100 cm. The distance of dm is specific to the beam energy and is verified by the clinic during commissioning. It's typical to use a farmer chamber for these measurements. At OHSU and for this study, the PTW waterproof 30013 Farmer® Ionization Chamber was used and operated at 300 V for all ion chamber measurements.

3. Methods

3.1 TBI Protocol

Planning by both the TPS and hand calculations assumed the same prescription and setup. The prescription was 1200 cGy to the mid body in 8 fractions. The mid body was defined at the level of the umbilicus, centered in both the coronal and sagittal planes. On the TBI phantom, the mid body location was centered along the same planes and 15 cm from the base of the inferior end. The mid body location was placed along the central axis of the beam, unless noted otherwise, and the distance from the source was 562.5 cm.

Each plan contains two fields that are parallel opposed. The gantry was oriented horizontally parallel to the floor. In the TPS, to create parallel opposed beams, one gantry angle was at 90° for the first field and the other was at 270° with the patient orientation not changing. The collimator was rotated to 45° for all fields. The field is fully opened to 40 cm x 40 cm at an SSD of 100 cm. For simplicity, all measurements were of only a single field of one fraction. These measurements were compared to single field calculations from the TPS and by hand. A fraction has a prescription of 150 cGy and the individual fields deliver 75 cGy the prescription point.

There were two different orientations utilized during planning. It's common to treat with a beam in the AP and another PA direction which we refer to as APPA setup. In this setup, the patient lies in the decubitus position. The lungs are shielded using lung blocks with a thickness of 2 HVL for half of the fractions. Another setup that was utilized was laterally opposed beams. The patient lays supine and the beam crosses that patient laterally. These patients require no lung shielding but otherwise have the same procedure.

For the purposes of this study, missing tissue compensation was not incorporated into either plan type.

3.2 Patient Selection

A total of 6 different patients were selected for this study. There was a relatively simple selection criteria. As part of their typical treatment, many TBI patients have a CT scan taken of their abdomen and thorax. Patients were eligible for this study if both of these regions were scanned in a single acquisition from the neck to the top of the pelvis. Patients were prioritized based on their size. Size was specified as thickness at the prescription point in the direction parallel to the beam central axis. Patient sizes ranged from pediatric patients to varying sized adults. No minimum or maximum constraint on size was imposed.

3.3 Phantom Setup

There was a custom TBI phantom used for all phantom dosimetry. The Phantom consisted of two sections setup to mimic patient scattering conditions for TBI treatment. The inferior section was composed entirely of solid water with a square cross-section of 30 cm in each direction and a thickness of 25 cm. For ion chamber measurements, this thickness of the inferior end was changed to match distances measured from patient plans on their CT images. The superior section is composed of 3 cedar planks with a cross-section of 27 cm x 29 cm, a total of 11cm thick, and surrounded on each side by 7 cm of solid water. The cedar planks mimic the low density of the lungs while solid water is a practical substitute for soft tissue.



Figure 4 Setup of phantom used in film and ion chamber dosimetry as well as in TPS and hand calculations. Labeled with inferior and superior sides that are referenced as well as some dimensions of total thickness and thickness of cedar section.

3.4 Eclipse Treatment Planning

The TPS used in this study was Eclipse™ and calculations were performed using its Acuros® XB version 15.6 dose algorithm. Plans were created in the TPS using CT images acquired prior to this study. The CT images for all patients were acquired using a 5mm slice thickness and imported directly into Eclipse™. There were four adult plans created all with the APPA orientation with an 18 MV beam. There were also four plans created from pediatric images. Two of these plans were in the APPA orientation, one using a 6 MV beam and the other a 10 MV beam. The other two pediatric plans were oriented in the lateral setup with a 6 MV beam. One extra plan was created solely on the TBI phantom with all of the other conditions kept the same as the adult patients.

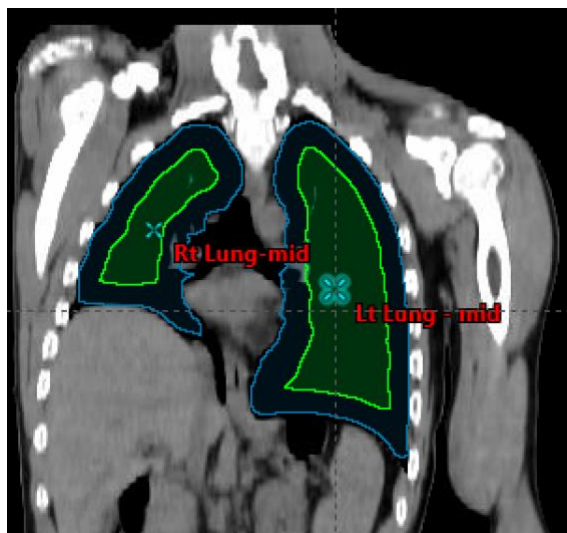


Figure 5: Contour of lungs in blue and contour of lungs minus 1.5 cm margin in green with reference points centered in both right and left lungs.

Lungs were contoured using patient CT images. For the plan created on the TBI phantom, a rectangular volume was contoured centrally within the cedar region of the phantom instead of actual anatomy. The volume contoured was roughly the same as the observed single lung volume of the adult patients. The lung contours were used to create a template for the lung blocks for APPA setups.

It's common to remove a margin from the lung contour prior to creating this template. This margin typically is used to prevent underdosing tissues surrounding the lungs. For adult patients at OHSU, this is typically 1 to 1.5 cm. For all but one plan created in this study, a 1.5 cm margin was removed. One exception was for planning on an infant. The lungs were not sufficiently large to remove this margin so it was decreased to 0.5 cm.

Lung blocks generated by the TPS are specific to both the beam direction (AP or PA) and patient lung geometry. In the TPS plans, lung blocks are automatically aligned to anatomy and placed on the tray attached to the linac head at an SSD of nearly 56 cm. This SSD is not adjustable in Eclipse™. During beam delivery, however, these are

attached to the spoiler which is placed at an SSD of 510 cm. Lung blocks were only implemented in 4 of the 8 fractions for APPA fields and not incorporated in lateral patient setups.

The prescription and TBI plan as previously described was applied to each patient plan. The calculation resolution for each plan was 0.25 cm and the dose reporting was dose to medium. Each patient had a dose point centered in each lung and at the prescription point. These supplied point dose estimates in these regions. The TPS also provides a mean lung dose of contoured anatomy. This was applied to both of the lungs which were separately contoured.

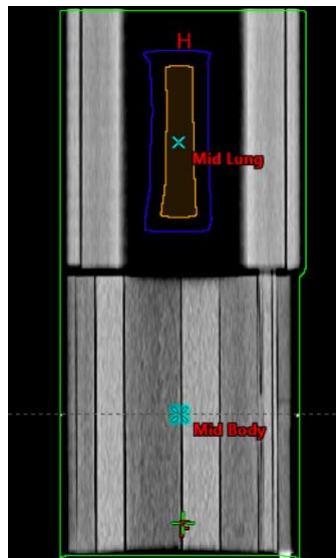


Figure 6: Cross-section of TBI phantom with lung contour in blue and lung contour -1.5cm in orange as well as mid lung and mid body reference points.



Figure 7: Example of the orientation of the lung blocks with respect to patient body. Cerrobend blocks are aligned to the lungs using CR imaging techniques and placed on the spoiler at a distance of 510 cm from the source during beam delivery.

For some patients, a plan was transferred onto the TBI phantom for only one of the AP fields with and without the lung blocks. These were intended to be used to compare to dose measurements. This was done using the patient quality assurance procedure in which patient CT images are substituted for images of the phantom. In this procedure all field information is kept the same including the MU's and shielding.

Some manual adjustments were necessary to center lung blocks over lung region of the phantom in the patient's inferior-superior direction and ranged from 0 to 10 cm. This central axis relocation was applied for all measurements compared to TPS predictions. For the initial treatment plan, reference points were also placed at the center of each lung. Both the TBI phantom and the initial plan had a reference point placed at the mid body location in the phantom. This is centered within the inferior section of the phantom that represents the abdomen.

3.5 Hand Calculations

All hand calculations followed the procedure in place for TBI treatment by OHSU. The assumed setup and the prescription are the same as described in the TBI procedure section. Calculations are done using a Tissue Maximum Ratio (TMR) method to estimate the number of MUs per field. Equations 1 and 2 represent the calculation used to find the dose rate (\dot{D}) in cGy/MU at the prescription point and MUs required (μ) to deliver a prescription dose (D). A number of other factors are used to correct for various effects including the inverse square factor (ISF), collimator scatter factor (S_c) for a 40x40cm field, phantom scatter factor (S_p) for a 26 x 26 cm field, spoiler factor, the normalization dose rate (D_0), and the TMR ratio itself for a 26 x 26cm field. A field size of 26 x 26 cm was used for both the S_p and TMR factors because that is the equivalent field size of an adult patient. Dose to a location is calculated using equation 4 which is the multiplication of the dose rate to the number of MU's. Methods are consistent for off-axis calculations of the head, neck, pelvis, etc.

$$\dot{D} = TMR \times ISF \times S_c \times S_p \times Tray \times Spoiler \times D_0 \quad \text{Eq.1}$$

$$\mu = \frac{D}{\dot{D}} \quad \text{Eq. 2}$$

$$ISF = \left(\frac{100+d_m}{562.5} \right)^2 \quad \text{Eq. 3}$$

$$D = \dot{D} \times \mu \quad \text{Eq.4}$$

Variable	Definition
\dot{D}	Dose rate (cGy/MU)
D	Dose (cGy)
D_0	Dose rate at d_m for 100 cm SSD and 10 cm square field (1 cGy/MU)
d_m	Depth of dose maximum
TMR	Tissue Maximum Ratio
S_c	Collimator scatter factor
S_p	Phantom scatter factor
Tray	Tray factor

Spoiler	Spoiler factor
ISF	<i>Inverse Square Factor</i>
μ	Monitor Units

Table 1: List of variables used for hand calculations in TBI treatment planning

The TMR ratio depends on field size and depth. Field size is considered uniform for each location but depth varies by sight thickness. For every location beside the lungs, this is half the physical distance measured with calipers of the selected anatomy. For the lungs, this changes slightly. The lungs are significantly less dense than water, so a water equivalent distance (WED) is used. This is a distance retrieved from the Eclipse™ TPS. It is the distance in water required to cause the same level of attenuation as in the physical material. This accounts for tissue inhomogeneities that can be substantial in the vicinity of the lungs compared to other locations. The WED is substituted for the depth in the lung TMR calculation. The remaining calculations are the same as before. It should be noticed that there is not a correction for off-axis measurements or decreased backscatter and lateral scatter. This is in line with the clinical procedure at OHSU and therefore was not adopted for this study.

3.6 Lung Block Fabrication

This study focused on patient CT data as well as planning directly on the TBI phantom. The creation of the lung blocks for patient-specific plans and on the phantom varied only in the shape of the block. For the TBI phantom, a CT scan was performed and uploaded into eclipse™ TPS. This allowed for contouring and dosimetry to be performed on patient images. On patient CTs, the lungs and body were contoured. On the TBI phantom, a rectangular volume of 1126 cm³ was contoured in the region occupied by cedar planks to represent a typical lung volume seen in patient samples. In both cases, a

second contour was made of the lungs that removed a 1.5 cm margin as previously described.

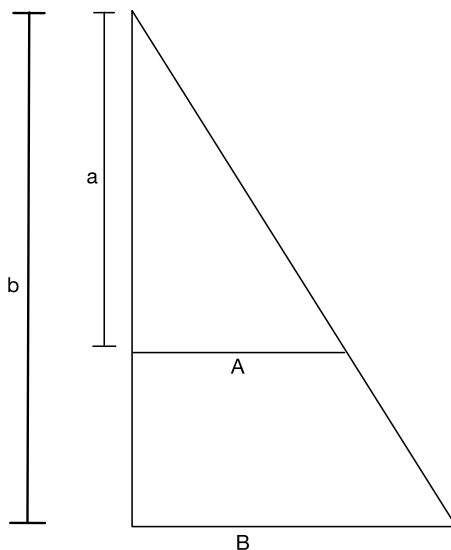


Figure 8: Similar triangles diagram.

$$\frac{A}{a} = \frac{B}{b} \text{ Eq. 4 Law of Similar Triangles [14]}$$

Lung blocks are shaped according to the CT contours. A template can be printed from Eclipse™ that matches the contour edges from a beam's eye view. This allows for scaling of the lung blocks that corrects for beam divergence. This scaling would reflect the distance from the source where the lung blocks will be placed in front of the patient. At OHSU, the distance from the source to the blocks is 510cm. Size is scaled using the law of similar triangles. This ensures that at mid body, the lung block projection would fit the anatomy. Scaling of the lung blocks could be verified by measuring graticule lines also printed on the template. No compensation besides lung blocking was added to plans.

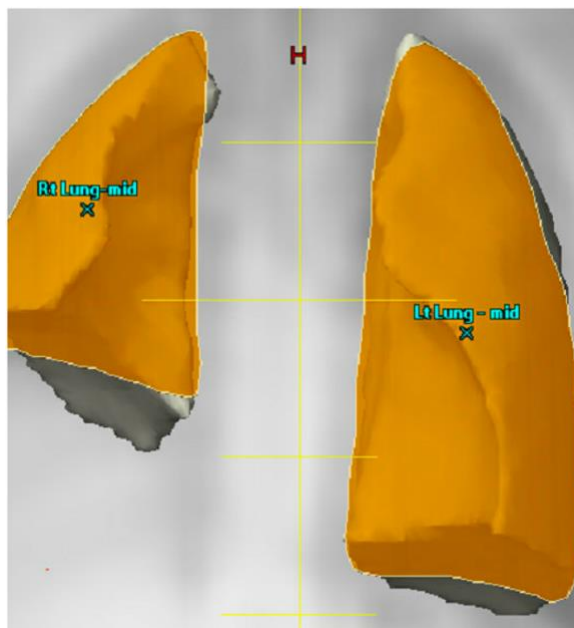


Figure 9: Example of printed lung block template used to create block forms shown in orange and graticule lines in yellow.

Molds were cut out of foam using the templates. The foam molds would then be filled with cerrobend. The standard thickness of 2 HVL was used for the lung blocks and a spoiler and tray were added to all plans. The HVL thickness of cerrobend was obtained from OHSU TBI commissioning data. For a 6 MV beam, this is 3.8 cm, for 10 MV beams it is 4cm, and for 18 MV beams it is 4.2 cm.

3.7 Ion Chamber Dosimetry

3.7.1 Chamber Calibration

The farmer chamber was used for all ion chamber measurements. The chamber was operated at 300 V set on the electrometer. On the day of measurement, the farmer chamber was exposed to a reference dose to create a dose per charge conversion. For each commissioned photon energy, OHSU machines are calibrated at 1 cGy per MU at d_m in water at an SSD of 100 cm and a field size of 10 cm x 10 cm. For each energy used in this study, the chamber was placed at d_m inside solid water with a square cross-section

of 30 cm x 30cm. A thickness greater than 10 cm of solid water was maintained beyond the ion chamber depth. The standard calibration setup was set for both 6 MV and 18 MV beams and 200 MU was delivered by the linac. This delivered 200 cGy to the chamber and allowed for the creation of a conversion factor from charge to dose using the charge recorded by the electrometer.

3.7.2 Stem and Cable Effects

During phantom irradiation, it was unavoidable that a significant portion of the cable was going to be in the radiation field. To verify variations in measured charge are insignificant, reference measurements were made. The ion chamber was left at 3.2cm depth in solid water for both energies (6MV and 18MV). The SSD was set to 100cm and the field size was 30 cm x 30 cm. First, 200 MU was delivered without the cord in the field and the charge was recorded. We then estimated the amount of cable that will be in the field during TBI measurements at extended SSD and marked the cable. That cable length was then placed on top of the phantom as shown in figure 9. Again, 200 MU was delivered and the charge was recorded. For both fields, there were 3 different measurements taken. The average charge collection for the field with and without the cable was then compared as a percentage.

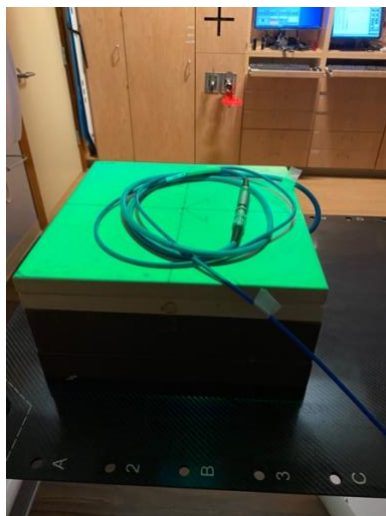


Figure 10 Measurement of charge with the stem and cable in the field during irradiation to verify the significance of stem and cable effects. Not visible in the photo, the farmer chamber is placed at the center of the field at a depth of 3cm. The dose was not derived from this reading. The charge reading was compared with and without the cable in the field.

3.7.3 Ion Chamber Phantom Measurements

The TBI phantom was placed in the typical setup. The distance from the source to the center of the phantom was set to 562.5cm and the field was opened fully to 40 cm x 40 cm and the collimator was rotated diagonally to 45 degrees. The acrylic spoiler was placed at 510 cm, the standard distance at OHSU, and the acrylic compensator was attached to the linac head. All measurements were at the mid body point of the phantom. The chamber was aligned in the center of the field according to markers from the linacs light field. The Depth and phantom thickness were based on patient CT images. Thickness was only varied at for the body section and the lung section remained unchanged. MUs delivered were according to planning on CT from the Acuros® model. Each TPS plan contained parallel opposed beams. The MUs from a single field was delivered to the phantom. The path of the beam is indicated by arrows in figure 10. The total charge was recorded and the charge to dose factor derived during calibration was applied to obtain the dose delivered.



Figure 11: The TBI phantom with the lung and body sections labeled. The yellow arrows indicate the path of the beam through the phantom.

3.8 Film Dosimetry

3.8.1 Film Calibration

Film dosimetry requires that a range of reference strips are irradiated for calibration. Our TBI treatments are modeled off of a 1200 cGy prescription to the mid body split between 8 fractions. This provides a dose of 150 cGy at the mid body reference point for each fraction with considerably less behind blocked areas of the lung. If one field is delivered, the dose to the mid body should be about 75 cGy. This information was used to select the range of reference strips to be irradiated.

Reference strips were cut to approximately 2 cm x 2 cm. An energy of 18MV was used for all film measurements. The radiochromic film used doesn't show significant energy dependence and a second calibration for 6 MV was not necessary. Similar to ion chamber calibration, reference strips were placed at d_m (3.2cm) in solid water with a 10

cm x 10 cm field and 100 cm SSD. With this setup, MU's can be equated to cGy deposited on the strips. Samples of 0, 25, 50, 75, 100, 150, 200, 250, and 300 cGy were irradiated. Closer intervals between 0 to 100 cGy were selected to create higher energy resolution at the dose levels we expected to see behind the lung blocks in a single field. Calibration strips were not irradiated before each trial. Instead, a test strip of either 100 cGy or 150 cGy was irradiated using the same setup to check the validity of the calibration file.

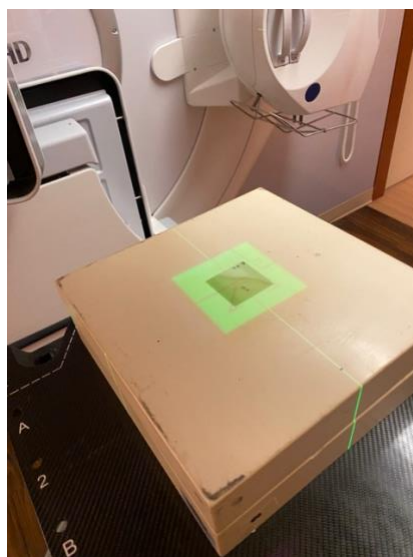


Figure 12: One of the films used for reference dosimetry during the processing of the strips placed in TBI phantom. This film would then have 3.2cm of solid water placed on top and irradiated to one of the listed calibration dose levels. This setup was also used for subsequent trials to verify the accuracy of the initial reference dose to avoid creating new dose conversion files for reading on separate days.

3.8.2 Phantom Measurements

The phantom used for film irradiation was the TBI phantom previously described. Unlike the ion chamber measurements, the phantom was maintained at dimensions of its standard size with a 25 cm thickness in all locations along the beams path. The spoiler and compensator were setup up as described for ion chamber phantom measurements. The lung blocks were attached to the linac side of the spoiler at an SSD of 510cm. Plans

previously calculated on the TPS were used to determine the number of MUs to deliver and which energy photon beam to use.

The phantom has no anatomy to reference during lung block positioning. The TPS was referenced to attempt to maintain the same spacing between lung blocks as planned. Prior to the radiochromic film being placed in the phantom, the position and spacing of the lung blocks were verified using CR port film. For the plan created on the phantom CT images, there was only one lung block and CR imaging was not necessary. The CR images allowed the magnification to be checked using the law of similar triangles.

It's crucial to maintain the same orientation of the radiographic film. A marking is made when it comes out of the factory packaging. Orientation with respect to the beam was also maintained using the initial marks. Because three cedar planks were used, it was not possible to place film at the central location of the lung section. Instead, there was an approximately 3 in x 6 in strip placed both anteriorly and posteriorly to the center cedar plank. A template was used to maintain a similar position on cedar planks for the strips placed in the lung section. Another approximately 2 in x 2 in film strip was placed at the mid body, centered on the solid water. This film had 12.5 cm of solid water both anterior and posterior to its position. This represents the prescription point of a TBI treatment.



Figure 13: The calibration films are shown with arrow markings indicating initial orientation when removed from factory packaging. These arrows are used to maintain consistent orientation while being scanned.

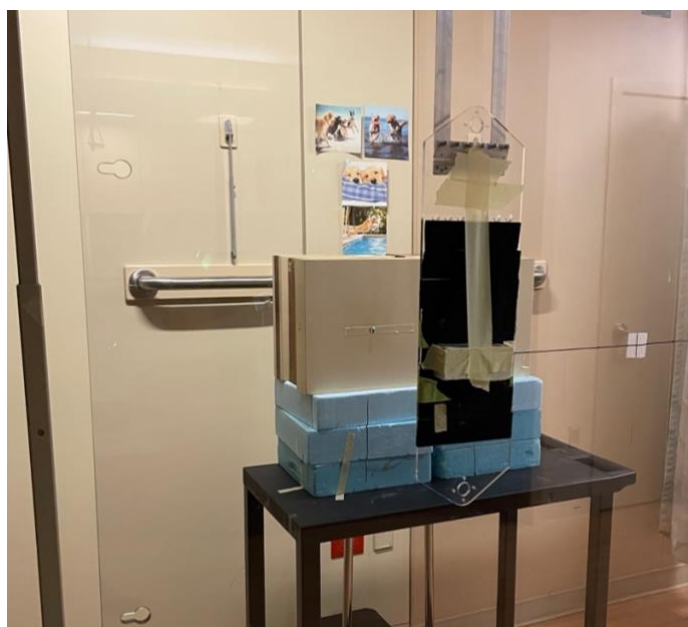


Figure 14: The TBI phantom is positioned for irradiation. In the beam path is the cerrobend block positioned to shield the central portion of the superior section of the phantom. The block pictured is the rectangular design created for the plan created directly on the TBI phantom. The block is fastened to the acrylic spoiler using Velcro attached to a mount at an SSD of 510 cm.



Figure 15: Pictured is a side view of the TBI phantom with the location of the film placement represented by red markers. Film size varied but the upper two marks show the location of the larger films used to get profiles of blocked fields. The lower marker represents the location of the smallest film used that measures the dose at the prescription point.

3.8.3 Film Processing

A standard procedure was developed for film measurements. After irradiation, the film was stored in a dark location for 21 hours before processing. The radiochromic film was scanned on the flatbed scanner with the red color channel selected which is standard at OHSU for dose levels less than 10 Gy. The resolution of the scan was 72 dpi and with 48-bit color for three color channels. Care was taken to ensure orientation was kept the same for all scanned film. This was done using the marks made just after removing from the factory packaging. The Epson® software uses an unirradiated sheet of film as a template to create an ROI that determines the size and location of the saved image as well as doing a uniformity correction in a later step. After the ROI is specified, each film is scanned and saved in full color as a “.tif” file.

Image processing was done using DoseLab software. Using this software, all film images are first converted to an optical density file which converts images from color to

black and white. The previously described calibration film strips of 0, 25, 50, 75, 100, 150, 200, 250, and 300 cGy were used in DoseLab to automatically create a calibration file that can be applied to other strips with a maximum dose less than 300 cGy. DoseLab applies an algorithm that fits to the data points. Anything above the maximum dose of the reference strips is equated to 0 dose. This means any point over 300 cGy in this study would be automatically set to 0. This file was only created from initial measurements and its accuracy was checked for each subsequent day using a test strip of known dose value as previously discussed.

The calibration file was applied to each scanned optical density file to convert it to a dose file. The new file contained a red green blue (RGB) color scale to represent dose distribution. The software allows for single image analysis. In this modality, ROIs can be placed that provide information on the mean and median dose in the selected location. ROIs were placed on the film to correspond to mid lung, or mid body locations depending on the intended placement of the film. The mean doses from the ROIs were used for later analysis of results.



4. Results

Various factors were tabulated for the patients selected for this study. An effort was made to select patients of a variety of different sizes. Their size was determined by the separation at the level of the umbilicus. The minimum patient separation was a pediatric patient with a distance of 15.2 cm in the AP direction. This patient had a plan created with a 10 MV and a 6 MV beam. The maximum separation was an adult with 34 cm in the AP direction. There were two lateral setups created for pediatric patients and the separation ranged from 22.6 cm and 29.8 cm both planned with a 6 MV beam. Lung volumes were tracked for each patient and adult patient's volumes were used as a reference for the creation of the lung contour of the phantom plan, patient number 9. In total there were 9 plans created in the TPS from 6 different patients and one on the TBI phantom.

Patient Number	Energy (MV)	Orientation	Lung Blocks	Patient Separation (cm)	Total Lung Volume (cm ³)
1	18	APPA	Yes	27	3507.7
2	18	APPA	Yes	20	2553.4
3	18	APPA	Yes	34	2809.9
4	18	APPA	Yes	33	2535.7
5	10	APPA	Yes	15.2	395.6
6	6	APPA	Yes	15.2	395.6
7 [†]	6	Lateral	No	22.6	395.6
8 [†]	6	Lateral	No	29.8	617.2
9 ^{††}	18	APPA	Yes	25	1126.2*

Table 2: Tabulation of beam energy, patient setup, shielding used, patient separation, and lung volume for each patient and patient plan created in the TPS and for hand calculations. The lung volume for patient 9^{††} is the rectangular contour of the TBI phantom.

Stem and cable effects were checked prior to the first farmer chamber measurements. The approximate length of cable that would be necessarily irradiated for TBI phantom measurements was evaluated in these measurements. Both 6 MV and 18 MV beams were used to irradiate the chamber and cable. For 18 MV beams and 6 MV

† Indicates lateral patient setup which does not contain lung shielding
 † † Indicates plan created on TBI phantom and not based on patient data
 : Indicates 10 MV beam used during planning and delivery
 : Indicates 6 MV beam used during planning and delivery

beams, there was a mean increase of 0.55% and 0.39% respectively in the total charge collected.

Energy	Stem and Cable Effect (%)
18 MV	0.55
6 MV	0.39

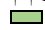

Table 3: Stem and cable effects for 6MV and 18MV beams when using the farmer chamber. The percent reported is the mean increase in charge collection when the cable is added to the field.

The TBI phantom was adjusted at the mid body to represent the thickness of 3 patients used in the TPS planning. This consisted of two adults using 18 MV beams and one pediatric patient setup using a 6 MV beam. The dose measured at the mid body location was compared to the predicted dose of 75 cGy using a hand calculation. Both 18 MV measurements showed a difference of -1.2% from the hand calculation prediction and the 6 MV measurement showed a 0.7% difference. The MUs reported are based on hand calculations. The MUs delivered to the phantom were scaled to match the hand calculation prediction to allow a dose comparison.

Patient Number	MU	Phantom Separation (cm)	% Dose Difference
1	2575	27	-1.2
2	2402	20	-1.2
6	2644	15.2	0.7

Table 4: Percent difference of dose measured by the farmer ion chamber at the prescription point with a varying phantom thickness to the dose predicted by hand calculations (75 cGy) on the TBI phantom. The phantom thickness was adjusted to match a patient's thickness from the TPS plans.

Plans were created on both Eclipse™ and using hand calculations. These plans were based on the same patient and allowed for the comparison of predicted MUs. The results for the patient-specific plans created using an 18 MV beam varied from 3.69% to 7.71% difference when comparing TPS prediction to hand calculations. The mean percent difference for these plans was 6.3% with a standard deviation of 2.2%. The plan created on the phantom with an 18 MV beam showed the lowest percent difference at -0.28%. The 10 MV APPA plan showed a difference of 2.44%. The 6 MV APPA plans

† Indicates lateral patient setup which does not contain lung shielding
 † † Indicates plan created on TBI phantom and not based on patient data
 : Indicates 10 MV beam used during planning and delivery
 : Indicates 6 MV beam used during planning and delivery

showed a mean difference of 4.00% with a standard deviation of 2.24%. The two Lateral 6 MV plans on the pediatric patients showed a difference of 2.65% and -0.43%.

Patient Number	Avg Eclipse MU	Hand Calc MU	MU % Diff
1	2774	2575	7.71
2	2553	2402	6.29
3	2991	2781	7.53
4	2851	2749	3.69
5	2555	2494	2.44
6	2750	2644	4.00
7 [†]	2911	2923	-0.43
8 [†]	3350	3263	2.65
9 ^{††}	2515	2522	-0.28

Table 5: Total monitor units predicted per field from both the Eclipse Acuros[®] algorithm and using hand calculation methods with a percent difference of Eclipse[™] MUs from that by hand calculations. The Acuros[®] prediction varied slightly between AP and PA beams so the average of the two was taken.

The WED from the TPS was used to calculate the dose to the lungs by hand when no shielding is used. For the same setup, the TPS prediction was compared to the hand calculation prediction. For this comparison, the hand calculation MU predictions were scaled to match the TPS prediction. The Eclipse Acuros[®] algorithm has a mean difference of -5.7% from hand calculations with a standard deviation of 2.4%.

Patient Number	MU	LL % Difference	RL % Difference
1	2795	-3.0	-4.5
2	2632	-3.7	-9.3
3	2944	-8.6	-8.5
4	2843	-4.2	-5.2
9 ^{††}	2646	-4.7	N/A

Table 6: Difference in lung dose predictions without lung shielding by Eclipse Acuros[®] algorithm from hand calculation predictions.

The TBI phantom was irradiated once without lung blocks. The dose at the mid lung was compared to predictions by the TPS on the TBI phantom. This required that the lung dose measurement be scaled based on MUs delivered and that predicted by the patient plan listed in the table below. The mean percent difference was 3.1% with a standard deviation of 0.4%. All film dose measurements were less than TPS predictions.

† Indicates lateral patient setup which does not contain lung shielding
 † † Indicates plan created on TBI phantom and not based on patient data
 ■ : Indicates 10 MV beam used during planning and delivery
 ■ : Indicates 6 MV beam used during planning and delivery

Patient #	MU	Film Dose (cGy)	Eclipses Dose (cGy)	% Difference
1	2795	82.6	85.4	-3.2
2	2632	77.8	80.6	-3.4
3	2944	87.1	89.9	-3.2
4	2843	84.1	86.9	-3.3
9 ^{††}	2646	78.2	80.2	-2.4

Table 7: Comparison of dose measured in lung region without lung blocks with Eclipse™ calculated dose on TBI phantom for an 18MV beam

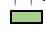

Film measurements were also compared to the dose predicted by hand calculations without lung shielding. For heterogeneity corrections, a WED was used for TMR calculations in the lung section of the TBI phantom. The film measurement was 7.0% lower than the hand calculation prediction.

Film dosimetry was used to evaluate the dose to the lung region and prescription point of the TBI phantom. Dose to the center of the phantom behind the lung blocks was tracked for both the right and left lungs. Film measurements were compared to patient plans that were transferred onto the TBI phantom. The numbers reported are corrected for differences in lung block attenuation from what was expected. The measured lung dose for both the right and left sides showed a mean difference of -18.6% and a standard deviation of 4.3% for the 18 MV plans and -20.3% and a standard deviation of 2.2% for the 6 MV plan when compared to the TPS prediction. The measurements to the prescription point on the phantom showed a mean difference of 0.9% and standard deviation 1.17% of for 18 MV plans and a difference of -0.5% for the 6 MV plan.

Patient Number	LL % Difference	RL % Difference	Mid Body % Difference
1	-20.0	-16.9	1.3
2	-13.0	-19.2	1.9
6	-18.7	-21.9	-0.5
9 ^{††}	-24.1	N/A	-0.4

Table 8: Percent difference of blocked Lung dose and mid body dose measurements from film on the TBI phantom compared to calculated values by the Eclipse Acuros® algorithm.

The TPS was used to compare the point dose to the mid lung as well as the mean dose to the whole lung. Large differences among energies were not noticed. This was

† Indicates lateral patient setup which does not contain lung shielding
† † Indicates plan created on TBI phantom and not based on patient data
 : Indicates 10 MV beam used during planning and delivery
 : Indicates 6 MV beam used during planning and delivery

analyzed by taking a ratio of mean lung dose to mid lung dose. The following data is for plans calculated in the APPA direction and including all fractions and fields. The mean of this ratio observed for 18 MV plans not including the phantom plan was 1.14. This ratio was 1.21 for the phantom plan. For 6 MV and 10 MV plans the mean of the ratio was 1.12 and 1.11 respectively.

Patient Number	TPS Mean/Mid L	TPS Mean/Mid R
1	1.12	1.17
2	1.10	1.18
3	1.16	1.11
4	1.11	1.18
5	1.12	1.10
6	1.12	1.11
9 ^{††}	1.21	N/A

Table 9: Comparison of mean to mid lung dose calculated by the Eclipse Acuros® algorithm on patient CT sim data of patient planned in the APPA beam direction setup. These comparisons are of dose accumulated from all fractions in the plan including blocked and unblocked fields.

A separate evaluation of the comparison of the mean to mid lung dose was made for pediatric lateral patient setups. In this setup, lung blocks are not utilized. The mean of this ratio was the lowest of all plans at 1.02.

Patient Number	TPS Mean/Mid L	TPS Mean/Mid R
7 [†]	1.02	1.04
8 [†]	1.00	1.01

Table 10: Comparison of mean to mid lung dose calculated by the Eclipse Acuros® algorithm using information from CT sim images of patients planned in the lateral beam direction setup. These are comparisons of dose accumulated from all fractions of the treatment plan.

† Indicates lateral patient setup which does not contain lung shielding
 † † Indicates plan created on TBI phantom and not based on patient data
 ■ : Indicates 10 MV beam used during planning and delivery
 ■ : Indicates 6 MV beam used during planning and delivery

5. Discussion

5.1 Findings

The results of this study show there is potential for the Eclipse Acuros® dose algorithm to be implemented as a clinical tool for TBI planning. The accuracy observed in the dose calculated at mid body as well as the unblocked lungs is within clinical standards with an average difference of 1% and 3% respectively. The target for whole body dose uniformity is $\pm 5\%$ [4]. The dose difference between our measurements and the TPS shows the potential to achieve this confidence.

Another study noted a greater deficit in dose prediction in a heterogenous material like the lung section of the TBI phantom [9]. That study used Styrofoam instead of dried cedar for their low-density material. This material choice may be the cause of their increased error [20]. Attenuation by the cedar planks may have a more equivalent to that encountered in the lungs and may suggest their study underestimates the ability of the Acuros® algorithm to handle heterogeneity corrections in a clinically relevant scenario.

In comparison with hand calculation, the TPS showed greater agreement to film measurements for unshielded lung dose. The film measured a 7% lower dose to the lungs than the hand calculations prediction, but only 3.1% lower than the TPS prediction on average. There wasn't enough variation in the measurements to draw a clear conclusion, but this does warrant further investigation. The dose to the unshielded lungs was consistently predicted to be higher by hand calculations. The TPS predicted a 5.7% lower dose on average than hand calculations for patient plans which correlates with the film measurements. The inability to account for changes in scattering conditions and the

minimal correction for tissue heterogeneity by hand calculations gives the TPS a clear advantage and likely causes hand calculations to over report the lung dose. Because of this, if a more complex anthropomorphic phantom is used, hand calculation would likely not improve to outperform the TPS for unshielded lung dose calculations.

Dissimilar to other results, the dose difference measured behind lung blocks showed significant differences from the TPS prediction. This measured difference ranged from 13% to 24% less than the predicted dose. This large deviation makes a clear conclusion difficult to draw. Our thoughts are that current methods of placing a lung shielding in the TPS are not sufficient for TBI planning. These results have been noted in another study and the degree of clinical significance is unclear [20].

The default in Eclipse™ is to place the blocks attached to the tray on the linac head like with other shielding used during radiotherapy. In reality, these blocks are located at a much farther SSD and closer to the patient. The blocks are scaled to still account for beam divergence to conform to the lungs but certain geometric effects like a penumbra are thought to play a role in causing this error. Eclipse doesn't allow for a quick adjustment of the shielding's mounting location and perhaps working with the vendor could help resolve this issue. Another possible method is to implement a bolus into the plan. The bolus can have its transmission adjusted to 2 HVL like the lung blocks but is located close to the skin surface.

The comparison of total MU's predicted by the TPS and hand calculations shows there are noticeable differences between the two methods. The largest differences were seen in the APPA plans created with an 18 MV beam with a mean 6.3% greater than hand calculations. Lower energy plans and specifically laterally positioned patients showed

more closely matching results. The plan on the TBI phantom showed a difference of only 0.3%. The phantom itself closely resembles the conditions that a TMR table is commissioned for TBI. Hand calculations are ideally suited for scattering conditions found in the mid body section of the TBI phantom. A closely matching calculation is expected in this instance. In the case of plans calculated on patient data, larger discrepancies are likely due to the inability to account for most tissue inhomogeneity and geometric differences in human anatomy by a hand calculation. A treatment planning system can account for these differences.

The TBI phantom was set up with varying thicknesses at the midbody to assess the difference in dose readings for different depths. In this case, the mid body was sized to resemble the thickness of a patient at the umbilicus. The MU's delivered varied slightly from what hand calculation predicted. A simple scaling factor was applied to the dose measurements to account for the MU difference. The measurements showed strong agreement with a mean difference of -0.6% from hand calculations. This method is similar to commissioning for TBI at an extended distance. This difference is within the expectation of clinical output and is representative of the validity of the applied hand calculation factors.

In clinics that monitor lung dose, it's typical for estimates to be reported as a point dose to the middle of the lung. This can sometimes be verified using *in vivo* dosimetry by taking entrance and exit dose readings [3 4]. This study primarily analyzed point dose measurements using film within the TBI phantom. During TBI planning, it's commonly preferred to use a point dose estimation because it is relatively easy to obtain. A 3-dimensional dose calculation is inherently more difficult because of the lack of a TPS

used in the planning stages. In this study, we evaluated the differences reported by the Eclipse Acuros® algorithm by comparing the mean lung dose to the point dose measurement in the mid lung. The mean dose was consistently higher with a minimum of 10% and a maximum of 18% higher with a mean of 13.6% higher for the patients oriented in the APPA setup. This is a finding consistent across energies. An exception to this is for laterally set up patients. These patient plans do not incorporate lung shielding so a greater degree of dose homogeneity would be expected. This is observed in the data and the greatest difference was 4%. It should be noted that the dose for lateral positioning was only calculated on pediatric patients and adults may see some differences because of increased lung volumes. Using a TPS in these instances to calculate a mean lung dose could provide useful insight into future studies and could warrant further investigation of this tool.

5.2 Limitations & Future Work

This study had inherent limitations that could be overcome in future studies. An anthropomorphic phantom would provide more reliable scatter conditions. Our phantom was simply constructed but was suitable for initial findings. The human trunk is more complex and less ideal. This could cause a difference in performance of the TPS that should be explored. This could apply to phantoms of varying sizes as well. We used one phantom size for plans, varying this size could uncover other issues or capabilities of the Eclipse Acuros® algorithm for TBI planning.

The large range in difference between measured dose and planned dose of the lungs behind shielding could be a result of many compounding factors. The manual process used to create lung blocks causes some variation in thickness. The thickness

difference causes some inequality in the attenuation of each block. Another consideration is the difference in lung size. Scattering contributions can be effected by broad beam geometry [14]. The variation in block size could be contributing to some of the error observed. This may justify investigating the creation of patient specific lung block thickness in future work.

OHSU has a relatively large sample of TBI patients but was limited in patients that met the criteria needed for this study. Coordination with other departments or programs to provide a greater sample of patients would help strengthen the results.

Only available resources and common planning techniques were employed. Exploring different planning techniques, specifically in fields using shielding, could improve inaccuracy of dose calculations. Potentially working with a vendor could help optimize this process and produce a more accurate plan. Minor changes to planning in another study have shown to improve some of this study's shortcomings.

In this study, missing tissue compensation was intentionally left out of planning and measurements. This was done out of simplicity and ease of measurements. In a future study, investigating its incorporation is critical. This type of compensation is necessary for patient treatment and its characterization is required if the TPS is to be used as the primary planning method.

6. Summary and Conclusion

Implementing a TPS for TBI treatment planning could have a profound clinical impact. Current treatment planning uses a hand calculation that is crude but thought to be sufficient for a positive patient outcome. This form of treatment planning lacks the ability to account tissue heterogeneity along with other patient specific parameters and is unable to provide a 3-dimensional dose distribution. We have investigated the ability of the Eclipse Acuros® dose calculation algorithm to handle an extended distance with scattering condition similar to those found in the human abdomen and thorax. The measurements involved allowed for a direct comparison to the performance of a hand calculation. The TPS was also used to evaluate the efficacy of a point dose estimate as a predictor of lung dose. This was accomplished by comparing the mid lung point dose to the mean lung dose, both of which are provided by the TPS.

The Eclipse Acuros® dose calculation algorithm has shown mixed results in its ability to be clinically useful for extended SSD applications like in TBI. On the TBI phantom, the algorithm performed well when applied to an unblocked field. When compared to dosimetry measurements, it showed it is capable of achieving a clinically relevant accuracy. This was apparent in the results for both mid body and lung region dosimetry in the phantom. This, however, cannot be stated for fields when lung shielding is utilized. The inability to exactly match the TBI setup in the eclipse software leaves some ambiguity in the TPS's ability in these circumstances. These uncertainties warrant further investigation into alternate planning techniques within the TPS.

For each patient plan, the TPS predicted a lower dose to the lungs than hand calculations. The hand calculation's inability to account for differences in scatter

condition and minimal tissue inhomogeneity corrections is likely responsible for this. Though both the TPS and hand calculations overestimated the dose measured on the TBI phantom, the TPS had a significantly closer result. Further investigation is needed to draw a conclusion but it's unlikely that in a more complex phantom hand calculations would increase in accuracy if no other corrections are applied.

The TPS showed a noticeable difference in its MU calculations compared to hand calculations as well. Taking into account the TPS's ability to calculate unblocked fields, this again may be a result of hand calculations shortcoming in accounting for the difference in scattering within the human body. Moreover, the mean lung dose predicted by the TPS showed a considerable deviation from the mid lung dose estimate. In reality, this could provide meaningful information for future research and is a good justification for why a TPS-based plan would be superior to a hand calculation. Using a TPS as the main MU calculation hasn't been yet shown to be feasible. Using a TPS as a second calculation does however provide information unattainable with current methods and could be a practical use if further work can create satisfactory results for lung dose estimates during blocked fractions.

Works Cited

[1-5 7-9 11-13 15-19 21 22]

1. Chao ST, Dad LK, Dawson LA, et al. ACR-ASTRO Practice Parameter for the Performance of Stereotactic Body Radiation Therapy. *Am J Clin Oncol* 2020;**43**(8):545-52 doi: 10.1097/coc.0000000000000706.
2. Almond PR, Biggs PJ, Coursey BM, et al. AAPM's TG-51 protocol for clinical reference dosimetry of high-energy photon and electron beams. *Med Phys* 1999;**26**(9):1847-70 doi: 10.1118/1.598691.
3. Galvin JM. Total Body Irradiation Dosimetry and Practical Considerations. Secondary Total Body Irradiation Dosimetry and Practical Considerations.
4. Dyk JVG, J. M.; Glasgow, G. P.; Podgorsak, E. B. THE PHYSICAL ASPECTS OF TOTAL AND HALF BODY PHOTON IRRADIATION. American institute of Physics 1986.
5. Quast U. Whole body radiotherapy: A TBI-guideline. *J Med Phys* 2006;**31**(1):5-12 doi: 10.4103/0971-6203.25664.
6. Volpe AD, Ferreri AJMa, Annaloro C, et al. Lethal pulmonary complications significantly correlate with individually assessed mean lung dose in patients with hematologic malignancies treated with total body irradiation. *International Journal of Radiation Oncology*Biography*Physics* 2002;**52**(2):483-88 doi: [https://doi.org/10.1016/S0360-3016\(01\)02589-5](https://doi.org/10.1016/S0360-3016(01)02589-5).
7. Scobioala S, Eich HT. Risk stratification of pulmonary toxicities in the combination of whole lung irradiation and high-dose chemotherapy for Ewing sarcoma patients with lung metastases: a review. *Strahlenther Onkol* 2020;**196**(6):495-504 doi: 10.1007/s00066-020-01599-8 [published Online First: 20200312].
8. Quast U. Total body irradiation--review of treatment techniques in Europe. *Radiother Oncol* 1987;**9**(2):91-106 doi: 10.1016/s0167-8140(87)80197-4.
9. Lamichhane N, Patel VN, Studenski MT. Going the distance: validation of Acuros and AAA at an extended SSD of 400 cm. *J Appl Clin Med Phys* 2016;**17**(2):63-73 doi: 10.1120/jacmp.v17i2.5913 [published Online First: 20160308].
10. Khan FM. *The Physics of Radiation Therapy*. 4th ed, 2010.
11. Constantinou C, Attix FH, Paliwal BR. A solid water phantom material for radiotherapy x-ray and gamma-ray beam calibrations. *Med Phys* 1982;**9**(3):436-41 doi: 10.1118/1.595063.
12. Ohkubo H, Kanemitsu Y, Uemura T, et al. Normal Lung Quantification in Usual Interstitial Pneumonia Pattern: The Impact of Threshold-based Volumetric CT Analysis for the Staging of Idiopathic Pulmonary Fibrosis. *PLoS One* 2016;**11**(3):e0152505 doi: 10.1371/journal.pone.0152505 [published Online First: 20160331].
13. Bush K, Gagne IM, Zavgorodni S, Ansbacher W, Beckham W. Dosimetric validation of Acuros XB with Monte Carlo methods for photon dose calculations. *Med Phys* 2011;**38**(4):2208-21 doi: 10.1118/1.3567146.
14. McDermott PN, Orton CG. *The Physics and Technology of Radiation Therapy*: Medical Physics Publishing, 2018.

15. Butson MJY, Peter K.N; Cheung, Tsang; Metcalfe, Peter. Radiochromic film for medical radiation dosimetry. *Materials Science and Engineering: R: Reports* 2003;**41**:61-120.
16. Bassi S, Cummins D, McCavana P. Energy and dose dependence of GafChromic EBT3-V3 film across a wide energy range. *Rep Pract Oncol Radiother* 2020;**25**(1):60-63 doi: 10.1016/j.rpor.2019.12.007 [published Online First: 20191209].
17. Lewis D, Micke A, Yu X, Chan MF. An efficient protocol for radiochromic film dosimetry combining calibration and measurement in a single scan. *Med Phys* 2012;**39**(10):6339-50 doi: 10.1118/1.4754797.
18. Niroomand-Rad A, Blackwell CR, Coursey BM, et al. Radiochromic film dosimetry: recommendations of AAPM Radiation Therapy Committee Task Group 55. American Association of Physicists in Medicine. *Med Phys* 1998;**25**(11):2093-115 doi: 10.1118/1.598407.
19. Knoll Gf. *Radiation Detections and Measurment*. 4gth ed: John Wiley & Sons, Inc., 2010.
20. Russell L, Sillanpaa J. Computational and Experimental Approaches for Evaluating Dose under a Block in TBI Geometry. *International Journal of Medical Physics, Clinical Engineering and Radiation Oncology* 2022:77-83 doi: 10.4236/ijmpcero.2022.111007.
21. Lamichhane N, Studenski MT. Improving TBI lung dose calculations: Can the treatment planning system help? *Med Dosim* 2020;**45**(2):168-71 doi: 10.1016/j.meddos.2019.09.004 [published Online First: 20191112].
22. Zeng Q. Evaluation of the Total Body Irradiation Treatment Planning Using Eclipse, 2019.
23. Devic S, Seuntjens J, Sham E, et al. Precise radiochromic film dosimetry using a flat-bed document scanner. *Med Phys* 2005;**32**(7):2245-53 doi: 10.1118/1.1929253.
24. Arjomandy B, Tailor R, Anand A, et al. Energy dependence and dose response of Gafchromic EBT2 film over a wide range of photon, electron, and proton beam energies. *Medical Physics* 2010;**37**(5):1942-47 doi: <https://doi.org/10.1118/1.3373523>.
25. Menegotti L, Delana A, Martignano A. Radiochromic film dosimetry with flatbed scanners: a fast and accurate method for dose calibration and uniformity correction with single film exposure. *Med Phys* 2008;**35**(7):3078-85 doi: 10.1118/1.2936334.
26. Micke A, Lewis DF, Yu X. Multichannel film dosimetry with nonuniformity correction. *Med Phys* 2011;**38**(5):2523-34 doi: 10.1118/1.3576105.
27. Wolden SL, Rabinovitch RA, Bittner NH, et al. American College of Radiology (ACR) and American Society for Radiation Oncology (ASTRO) practice guideline for the performance of total body irradiation (TBI). *Am J Clin Oncol* 2013;**36**(1):97-101 doi: 10.1097/COC.0b013e31826e0528.
28. Lu L. Dose calculation algorithms in external beam photon radiation therapy. *International Journal of Cancer Therapy and Oncology* 2013.
29. Luk SMH, Wallner K, Glenn MC, et al. Effect of total body irradiation lung block parameters on lung doses using three-dimensional dosimetry. *J Appl Clin Med*

Phys 2022;**23**(4):e13513 doi: 10.1002/acm2.13513 [published Online First: 20220105].